Inorg. Chem. **2006**, *45*, 9132–9136

Solid-State ^{119}Sn NMR and Mössbauer Spectroscopy of "Distannynes": Evidence for Large Structural Differences in the Crystalline Phase

Geoffrey H. Spikes,[†] Jason R. Giuliani,[†] Matthew P. Augustine,[†] Israel Nowik,[§] Rolfe H. Herber,[§] and Philip P. Power*

Department of Chemistry, University of California, Davis, California, 95616 and Racah Institute of Physics, The Hebrew University of Jerusalem, 91904, Jerusalem, Israel

Received June 2, 2006

The "distannynes" Ar′SnSnAr′ (Ar′ = C_6H_3-2,6(C_6H_3-2,6-Pr^i_2)$_2$) and Ar*SnSnAr* (Ar* = C_6H_3-2,6(C_6H_2-2,4,6-Pr^i_3)$_2$) were examined by solid-state ^{119}Sn NMR and Mössbauer spectroscopy. The two compounds display substantially different spectroscopic parameters, while differing only in the absence (Ar′SnSnAr′) or presence (Ar*SnSnAr*) of a para-Pr^i group in the flanking aryl rings of their terphenyl substituents. The spectroscopic differences can be interpreted in terms of a more trans-bent geometry and a longer Sn–Sn bond for Ar*SnSnAr* in comparison to the wider Sn–Sn–C angle (125.24(7)°) and shorter Sn–Sn bond length (2.6675(4)Å) determined from the crystal structure of Ar′SnSnAr′. The differences are consistent with previously published calculations by Nagase and Takagi for Ar*SnSnAr*.

Introduction

The use of sterically crowding ligands has enabled the isolation and structural characterization of the first stable examples of heavier group 14 element alkyne analogues.[1−6] In contrast to the lighter (i.e., carbon based) alkynes, they all have trans-bent rather than linear structures. Structural data for the terphenyl germanium,[3] and tin[2] derivatives Ar′MMAr′ (M = Ge or Sn; Ar′ = C_6H_3-2,6(C_6H_3-2,6-Pr^i_2)$_2$; Figures 1 and 2) showed that the structures are similar and have Ge−Ge and Sn−Sn bonds that are shortened with respect to single bond lengths, 2.44 Å (Ge) and 2.81 Å (Sn), and that they have wide M−M−C angles, as shown in Figure 2. Nonetheless, the experimentally measured structure of Ar′SnSnAr′ disagreed with the calculations of Nagase and co-workers on the closely related Ar*SnSnAr* derivative (Ar* = C_6H_3−2,6(C_6H_2−2,4,6-Pr^i_3)$_2$; Figure 3) in which the Ar* ligand differed only from the Ar′ ligand in that it had a Pr^i substituent at the para position of each of the flanking aryl rings of the terphenyl group (Figure 1).[7] In contrast, the calculations showed that there was a fair agreement between the experimental and the theoretical data for Ar′GeGeAr′ and Ar*GeGeAr*, as illustrated by a comparison

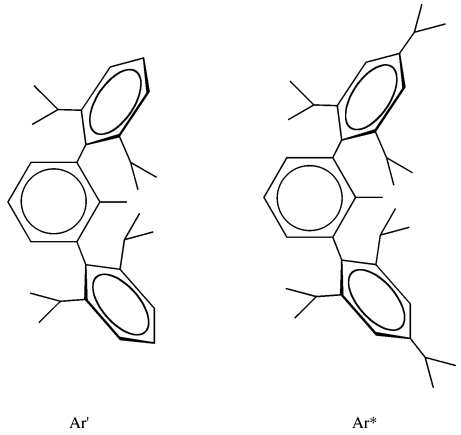

Figure 1. Schematic drawings of the Ar′ and Ar* ligands.

* To whom correspondence should be addressed. E-mail: pppower@ucdavis.edu.
[†] Department of Chemistry, University of California, Davis, California, 95616.
[§] Racah Institute of Physics, The Hebrew University of Jerusalem, 91904, Jerusalem, Israel.

(1) Pu, L.; Twamley, B.; Power, P. P. *J. Am. Chem. Soc.* **2000**, *122*, 3524.
(2) Phillips, A. D.; Wright, R. J.; Olmstead, M. M.; Power, P. P. *J. Am. Chem. Soc.* **2002**, *124*, 5930.
(3) Stender, M.; Phillips, A. D.; Wright, R. J.; Power, P. P. *Angew. Chem., Int. Ed.* **2002**, *41*, 1785.
(4) Wiberg, N.; Vasisht, S. K.; Fischer, G.; Mayer, P. *Z. Anorg. Allg. Chem.* **2004**, *630*, 1823.
(5) Sekiguchi, A.; Kinjo, R.; Ichinohe, M. *Science* **2004**, *305*, 1755.
(6) Sugiyama, Y.; Sasamori, T.; Hosoi, Y.; Furukawa, Y.; Takagi, N.; Nagase, S.; Tokitoh, N. *J. Am. Chem. Soc.* **2006**, *128*, 1023.
(7) Takagi, N.; Nagase, S. *Organometallics* **2001**, *20*, 5498.

10.1021/ic060983m CCC: $33.50
Published on Web 09/26/2006

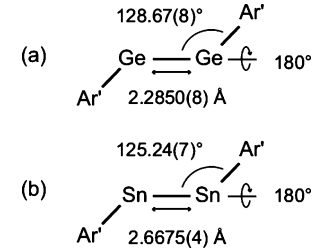

Figure 2. Summary of relevant measured structural data for Ar′GeGeAr′ (a)[3] and Ar′SnSnAr′ (b).[2]

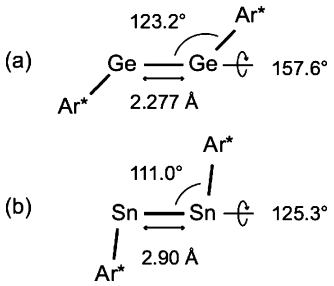

Figure 3. Summary of relevant calculated structural data for Ar*GeGeAr* (a) and Ar*SnSnAr* (b).[7]

of the calculated structure (Figure 3a) with the measured structure for Ar′GeGeAr′ (Figure 2a). In this case, the calculated Ge−Ge distance in Ar*GeGeAr* was close to that measured in Ar′GeGeAr′, although ca. 5° and ca. 24° deviations in the Ge−Ge bond and Ge−Ge−C twist angles, respectively, are recognized. The deviations in bond length, bond angle, and twist angle were much more severe in the case of the analogous tin derivatives Ar′SnSnAr′ and Ar*SnSnAr*. Comparison of the calculated structure[7] for Ar*SnSnAr* shown in Figure 3b to the measured structure for Ar′SnSnAr′ shown in Figure 2b revealed that theory predicts a ca. 0.2 Å longer Sn−Sn bond, a ca. 14° narrower Sn−Sn−C bond angle, and a ca. 55° deviation in twist angle around the Sn−Sn bond.

It is clear that the best test of theory in this main group metal atom structural problem is the structural characterization of the recently prepared Ar*MMAr* compounds.[8] Unfortunately, despite much effort, structural data could not be obtained because of the poor X-ray diffraction characteristics of the crystals of the Ar* substituted species. The availability of two $I = 1/2$ nuclear spins combined with the ability of Sn to absorb gamma rays in comparison to the $I = 9/2$ and gamma ray transparent Ge nucleus prompted the application of both ^{119}Sn solid-state NMR and Mössbauer spectroscopies to the crystals of Ar′SnSnAr′ and Ar*SnSnAr* to reconcile theoretical predictions.

Experimental Section

The compounds Ar′SnSnAr′ and Ar*SnSnAr* were prepared under anaerobic and anhydrous conditions as described in the literature.[2,8] The compounds were extremely air and moisture sensitive, and strict precautions were required to exclude contamination of the spectroscopic samples.

Solid-state ^{1}H decoupled ^{119}Sn nuclear magnetic resonance (NMR) experiments were performed at 109.9 MHz corresponding to a $\mathbf{B}_0 = 6.95$ T magnetic field using a home-built NMR console constructed around a Tecmag Orion pulse programmer. Although a Bruker magic angle spinning NMR probe was used with powdered solid samples contained in 4 mm outer diameter O-ring sealed zirconium oxide magic angle spinning rotors, all spectra were obtained without sample rotation as the ca. 40 spinning sidebands and the ca. 2000 ppm width of the spinning sideband manifold precluded application of the standard Herzfeld-Berger spinning sideband analysis to obtain the principal components of the chemical shift tensor.[9] Rather, the "spikelet" transform method[10,11] based on the signal measurement with the Carr−Purcell−Meiboom−Gill (CPMG) multiple π rf pulse sequence[12] was used. Here, Fourier transformation of the CPMG multiple echo signal yielded a ^{119}Sn spectrum of spikelets with an intensity envelope that described the ^{119}Sn powder pattern. The δ_{nn} ($n = 1$, 2, or 3) principal values of the chemical shift tensor were obtained using Matlab to fit the spikelet amplitude to the analytical form for an $I = 1/2$ chemical shift powder pattern. Furthermore, the δ_{nn} values were assigned with reference to tetramethyl tin at 0 ppm and with δ_{33} corresponding to the largest upfield shift consistent with ^{13}C δ_{nn} assignments for methylene carbons.

Temperature-dependent Mössbauer experiments were carried out in transmission mode[13] using a 2.5 mCi ^{119m}Sn/$BaSnO_3$ source at room temperature. Spectrometer calibration was accomplished by using a 20 mg·cm^{-2} α-Fe absorber. Isomer shifts are reported with respect to the centroid of the room-temperature $BaSnO_3$ spectrum. The as-received samples were transferred in an inert atmosphere glovebox to O-ring sealed plastic sample holders and immediately cooled to liquid nitrogen temperature. These cooled sample holders then were transferred to a pre-cooled cryostat and examined in transmission geometry. The full widths at half-maximum of 0.90 ± 0.01 mm·s^{-1} at 90 K and 0.86 ± 0.03 mm·s^{-1} at 130 K for Ar′SnSnAr′ and 0.89 ± 0.04 mm·s^{-1} at 230 K for Ar*SnSnAr* are in reasonable agreement with the natural line width of 0.644 ± 0.04 mm·s^{-1}. All temperature-dependent Mössbauer data were obtained in both warming and cooling mode, and no evidence of hysteresis was observed.

Results

All attempts to obtain liquid-state ^{119}Sn NMR spectra for either Ar′SnSnAr′ or Ar*SnSnAr* failed, while operation in the solid state yielded classic asymmetric spin $I = 1/2$ powder patterns because of the large ^{119}Sn chemical shift anisotropy. The three principal values of the shift tensor δ_{nn} ($n = 1$, 2, or 3) measured from the ^{119}Sn solid-state NMR spectra for both the Ar′SnSnAr′ and Ar*SnSnAr* compounds shown in Figure 4, panels a and b, respectively, are shown in Table 1 along with the average or isotropic chemical shifts $\delta_{iso} = (\delta_{11} + \delta_{22} + \delta_{33})/3$ and the powder pattern asymmetry parameters $\eta = (\delta_{22} - \delta_{11})/(\delta_{33} - \delta_{iso})$ calculated from these δ_{nn} values.

The Mössbauer spectra for both the Ar′SnSnAr′ and Ar*SnSnAr* compounds shown in Figure 5a and b, respec-

(8) Cui, C.; Olmstead, M. M.; Fettinger, J. C.; Spikes, G. H.; Power, P. P. *J. Am. Chem. Soc.* **2005**, *127*, 17530.

(9) Herzfeld, J.; Berger, A. *J. Chem. Phys.* **1980**, *73*, 6021.
(10) Siegel, R.; Nakashima, T. T.; Wasylishen, R. E. *J. Phys. Chem. B*, **2004**, *108*, 2218.
(11) Hu, J. Z.; Wind, R. A. *J. Magn. Reson.* **2003**, *163*, 149.
(12) Meiboom, S.; Gill, D. *Rev. Sci. Instrum.* **1958**, *29*, 6881.
(13) Adams, R. D.; Captain, B.; Herber, R. H.; Johansson, M.; Nowik, I.; Smith, J. L., Jr.; Smith, M. D. *Inorg. Chem.* **2005**, *44*, 6346.

Table 1. ^{119}Sn Solid-State NMR and Mössbauer Parameters for Ar′SnSnAr′ and Ar*SnSnAr*

		Ar′SnSnAr′	Ar*SnSnAr*
NMR	δ_{11}(ppm)	+1125.2	+726.1
	δ_{22} (ppm)	+740.4	+193.3
	δ_{33} (ppm)	−860.3	−1028.0
	δ_{iso} (ppm)[a]	+335.1	−36.2
	η[b]	0.32	0.54
	CSA[b]	−1793.1	−1487.7
Mössbauer[c]	IS (mm·s^{-1})	2.658(2)	2.69(3)
	QS (mm·s^{-1})	2.995(2)	3.730(3)
	d IS/dT (μm·s^{-1}·K^{-1})	−0.24(0.027)	−0.496(0.106)
	d QS/dT (μm·s^{-1}·K^{-1})	−1.98(62)	−2.52(7)

[a] The isotropic chemical shift is defined as $\delta_{iso} = (\delta_{11} + \delta_{22} + \delta_{33})/3$. [b] The asymmetry parameter is defined as $\eta = (\delta_{22} - \delta_{11})/(\delta_{33} - \delta_{iso})$; CSA (chemical shift anisotropy) $= 3/2(\delta_{33} - \delta_{iso})$. [c] The IS scale reference point is the centroid of a room-temperature absorption spectrum of BaSnO3.

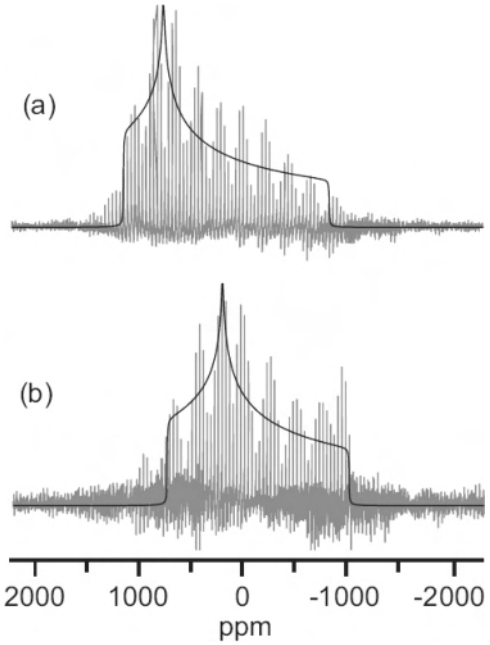

Figure 4. ^{119}Sn solid-state NMR spectra for Ar′SnSnAr′ (a) and Ar*SnSnAr* (b). The gray lines correspond to measured data, while the powder pattern fit is denoted by the solid black lines.

tively, contain a doublet at the isomer shift (IS) for Sn(II). The spectrum for the Ar′SnSnAr′ compound shown in Figure 4a has a small impurity with an intensity less than 10% of the major peak at 90 K as demonstrated by the fit solid lines. The impurity IS is appropriate for an Sn(II) contaminant, but further commentary on the identity of the compound is not possible at this time. The contribution of the impurity to spectral parameters was accounted for in the reported results. The measured IS and quadrupole splitting (QS) as well as their temperature dependences d IS/dT and d QS/dT measured at 12 points between 86 and 230 K for Ar′SnSnAr′ and at nine points between 86 and 160 K for Ar*SnSnAr* are provided in Table 1.

Discussion

Both the ^{119}Sn NMR and the Mössbauer sample holders were able to preserve the highly reactive Ar′SnSnAr′ and Ar*SnSnAr* compounds during the several day data acquisition period. In both cases, O-ring sealed samples were used to avoid reaction with air and water. The lack of any changes

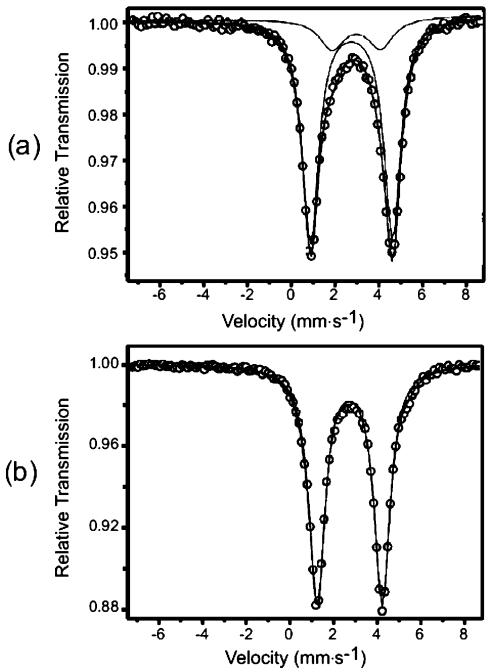

Figure 5. ^{119}Sn Mössbauer spectra for Ar′SnSnAr′ (a) and Ar*SnSnAr* (b) obtained at 90 K. The isomer shift scale is with reference to a room-temperature $BaSnO_3$ sample. The Sn(II) impurity in the Ar′SnSnAr′ sample gives rise to the smaller doublet curve described by the solid lines in (a).

in the ^{119}Sn solid-state NMR spectrum over the period of one month was one verification that the samples did not decompose. Additionally, both the color of the crystals and the ^{1}H liquid-state NMR spectra obtained for crystals removed from these sealed rotors and dissolved in deuterated benzene were consistent with the fresh sample that had not been stored in the O-ring sealed rotors. In the course of performing the Mössbauer experiments, it was noticed that a small amount of the colored Ar*SnSnAr* crystals rapidly turned white upon exposure to air. The IS $\approx$ 0 mm·s^{-1} and the broad resonance absorption of this white material was consistent with the formation of a tin(IV) oxide. A similar experiment was not performed on Ar′SnSnAr′ because of limited sample quantities, but it is reasonable to assume that this "distannyne" also will react with air to form tin(IV) oxide. No absorbance due to this IS $\approx$ 0 mm·s^{-1} tin(IV) oxide decomposition product was observed during the variable temperature Mössbauer measurement that required at least 8−24 h at each temperature point.

The next two sections discuss several aspects of the ^{119}Sn solid-state NMR and Mössbauer results related specifically to the Ar′SnSnAr′ and Ar*SnSnAr* compounds. The third and final section compares the ^{119}Sn solid-state NMR and Mössbauer results for each compound to each other to substantiate theoretical models of the Ar*SnSnAr* structure.

Ar′SnSnAr′. The distribution of the principal components of the chemical shift tensor δ_{nn} (n = 1, 2, or 3) reported in Table 1 is consistent with the reduced symmetry structure shown in Figure 2b. For example, consider the ^{13}C chemical shift tensor values for methane, acetylene, and ethylene.[14]

(14) Duncan, T. M. *A Compilation of Chemical Shift Anisotropies;* The Farragut Press: Chicago, IL, 1990.

The tetrahedral symmetry in solid methane yields one narrow NMR peak reflecting the equality $\delta_{11} = \delta_{22} = \delta_{33}$, while the cylindrical symmetry in solid acetylene produces an axially symmetric powder pattern in the solid state with two different principal components $\delta_{11} = \delta_{22}$ and δ_{33}. Both of these high-symmetry cases have $\eta = 0$. The third case involving solid ethylene gives an asymmetric powder pattern with $\eta \neq 0$ and three different principal axis components with $\delta_{11} > \delta_{22} > \delta_{33}$. The trans-planar structure for Ar′SnSnAr′ suggests that $\delta_{11} > \delta_{22} > \delta_{33}$ values should be measured in the ^{119}Sn solid-state NMR spectrum, and the $\eta = 0.32$ asymmetry parameter reflects the deviation of the structure shown in Figure 1b from cylindrical symmetry around the Sn−Sn bond. This is because the expression for η (see Table 1 legend) involves $\delta_{11} - \delta_{22}$ as the numerator. The difference between these values reflects the changes in the in-plane component (δ_{22}) relative to the out-of-plane component (δ_{11}) caused by trans bending. The surprising feature of these data is the $\delta_{iso} = +335.1$ ppm isotropic chemical shift for Ar′SnSnAr′ given that the oxidation state of tin is +2 and that Sn(II) containing molecules typically display $+500$ ppm $< \delta_{iso} < +4000$ ppm values, while the more highly shielded Sn(IV) compounds yield -500 ppm $< \delta_{iso} < +1000$ ppm values.[14−16] Although the isotropic chemical shift is somewhat lower than most two-coordinate diorgano Sn(II) compounds (usual range ca. $+700 < \delta_{iso} < +2300$ ppm),[15,16] the observed $\delta_{iso} = +335.1$ ppm chemical shift for the Ar′SnSnAr′ dimer is still substantially deshielded relative to the $\delta_{iso} = -290$ ppm chemical shift reported for the monomeric "singlet carbenoid" Sn(OAr′)$_2$ compound.[17] The -290 ppm isotropic chemical shift reported for Sn(OAr′)$_2$ is the most shielded value currently known for a two-coordinate Sn(II) species and is consistent with the back-bonding of the nonbonding electron pairs in the OAr′ ligand into the empty p orbital on tin. This is an effect that quenches the orbital angular momentum at tin thus reducing the paramagnetic contribution to the observed ^{119}Sn chemical shift.[18−19] In addition, the energy gap between the tin lone pair and the tin p orbital is increased by the highly electronegative OAr′ ligands thereby reducing the paramagnetic contribution to the chemical shift. This upfield trend of the ^{119}Sn chemical shift in two-coordinate Sn(II) species inversely correlates with ligand electronegativity values.[15−18] In the case of the tin dimer studied here, the SnAr′ group is a ligand to the other SnAr′ group, and there is a lone electron pair on tin that readily interacts with the empty p orbital on the second tin atom. The participation of the formally empty p orbital in the Sn−Sn chemical bond in the case of the Ar′SnSnAr′ dimer is consistent with ^{119}Sn NMR shift and the molecular structure.[19]

The IS value reported in Table 1 for Ar′SnSnAr′ obtained from the Mössbauer spectrum is consistent with Sn(II) and, as expected, decreases with increasing temperature. The slope of this linear decrease in IS, d IS/dT, is reported in Table 1. The temperature dependence of the recoil free fraction of the tin resonance for an optically thin absorber scales with the temperature dependence of the area A under the resonance curve. The slope of ln(A) versus T is linear with a correlation coefficient of 0.995 for 12 data points. This temperature dependence can be used[20] to calculate the root-mean-square amplitude of vibration at all temperatures and at 90 K corresponds to 0.110 Å, a value that compares well with the 0.133 Å value calculated from the X-ray data obtained at 91(2) K. Moreover, the $U_{i,j}$ X-ray values imply essentially isotropic vibrational motion of the Sn(II) atom at this temperature, which is in good agreement with the spectral area ratio of 1.005(9) observed in the 90 K Mössbauer data. The QS parameter is nearly temperature independent in the range $90 < T < 190$ K, but at higher temperatures, QS decreases with temperature, which is consistent with thermal lattice expansion. The ratio of the areas of each peak of the QS doublet to each other is temperature dependent, which indicates an asymmetry in the metal atom motion that is parallel and perpendicular to the principal symmetry axis of the molecule.

Ar*SnSnAr*. As shown in Table 1, a similar distribution of chemical shift principal component values was observed for Ar*SnSnAr*. These three different principal component values, combined with the $\eta = 0.54$ asymmetry parameter, are consistent with the more bent structure shown in Figure 3b as well as those observed in other reduced symmetry molecular systems. As mentioned above, the observed $\delta_{iso} = -36.2$ ppm chemical shift is also within the range established by Sn(OAr′)$_2$ and other two-coordinate Sn(II) compounds[15−18].

The IS reported in Table 1 for the Mössbauer spectrum for Ar*SnSnAr* unambiguously identifies the metal atoms as Sn(II). This sample also contains a small Sn(II) impurity, but it is only ≈3% of the total area under the resonance curve and was corrected in the data analysis. The maximum temperature explored in this sample was 160 K instead of the 230 K used for Ar′SnSnAr′ because the gamma ray absorption dropped below 0.76% at higher temperatures. Although the functional form of the IS temperature dependence between 90 and 160 K is not linear, an estimate of the size of the temperature effect is provided by the initial slope d IS/dT reported in Table 1. As usual, the QS parameter temperature dependence is negative in agreement with the thermal expansion effects on the field gradient experienced by the metal atoms. Finally, there is a minor temperature dependence of the intensity ratio of the Mössbauer doublet peak areas to each other within the 90−160 K temperature range, which again reflects the motional anisotropy of the metal atoms in this thermal regime.

Structural Implications. The ^{119}Sn NMR and Mössbauer data clearly indicate that the structures of Ar′SnSnAr′ and

(15) Wrackmeyer, B. *Ann. Rep. NMR. Spectrosc.* **1999**, *38*, 203.
(16) Marsmann, H. C.; Uhlig, F. In *The Chemistry of Organic Germanium, Tin, and Lead Compounds;* Rappoport, Z., Ed.; Wiley: New York, 2002; Vol. 2, Part 1, p 399 ff.
(17) Stanciu, C.; Richards, A. F.; Stender, M.; Olmstead, M. M.; Power, P. P. *Polyhedron* **2006**, *25*, 477.
(18) Eichler, B.; Phillips, B. L.; Power, P. P.; Augustine, M. P. *Inorg. Chem.* **2000**, *39*, 5450.
(19) Wiberg, K. B.; Hammer, J. D.; Zilm, K. W.; Keith, T. A.; Cheeseman, J. R.; Duchamp, J. C. *J. Org. Chem.* **2004**, *69*, 1086.
(20) Herber, R. H.; Nowik, I.; Kahlenberg, V.; Kopacka, H.; Schottenberger, H. *Eur. J. Inorg. Chem.*, in press.

Ar*SnSnAr* differ in the solid state. For example, the increase in the ^{119}Sn asymmetry parameter η, the decrease in the ^{119}Sn isotropic chemical shift δ_{iso}, and the decrease in the d IS/dT values upon the addition of a Pr^i ligand to change Ar′SnSnAr′ into Ar*SnSnAr* are consistent with a slightly stronger metal-to-metal interaction in Ar′SnSnAr′ compared to that in Ar*SnSnAr*. The difference probably arises because of the increased steric demand of the Ar* ligand which carries Pr^i groups at the para positions of the flanking aryl groups. Inspection of the structure of Ar′SnSnAr′ (and Ar′GeGeAr′) shows that the central aryl ring of the Ar′ ligands is coplanar with the C(ipso)SnSnC(ipso) core, and the flanking rings of the Ar′ ligands are essentially perpendicular to this plane. Molecular models show that this configuration would be disfavored if para Pr^i groups were present on the flanking rings. Thus, it seems very likely that Ar*SnSnAr* has a structure in which the central aryl rings of the Ar* ligands are oriented almost perpendicularly to the C(ipso)SnSnC(ipso) core. This view is supported by both experimental data and the known structures of related compounds. Specifically, the stronger metal-to-metal interaction in Ar′SnSnAr′ yields a molecule with less deviation from linearity than Ar*SnSnAr* and, thus, a smaller asymmetry parameter η and quadrupolar splitting QS. The lower bending in Ar′SnSnAr′ has the opposite effect on the isotropic chemical shift δ_{iso}, which is an observation that may be connected with recent calculations[19] for the model species MeSnSnMe which have shown that the HOMO−LUMO gap and orbital type are strongly affected by the degree of trans-bending. When the Sn−Sn−C angle is ca. 125° (Ar′SnSnAr′), the HOMO is a π level and the LUMO is an n_+ lone pair combination. When the Sn−Sn−C angle is <100°, the HOMO becomes n_+ and the LUMO is now an unoccupied π level and the HOMO−LUMO gap increases. This increased energy gap could account for the measured upfield shift for Ar*SnSnAr* in comparison to that of Ar′SnSnAr′. This molecular geometry change with ligand identity is echoed in the X-ray crystal structure of the corresponding lead species Ar*PbPbAr*, which has the central aryl ring oriented at an angle of 88.8° with respect to the C(ipso)-PbPbC(ipso) plane.[1] This structure also has a strongly trans-bent narrow Pb−Pb−C angle (94.26(4)°) and a long Pb−Pb bond of 3.1881(1) Å, and it is likely that the structure of Ar*SnSnAr* has similar characteristics in which there is essentially a single Sn−Sn bond. These arguments are consistent with the theoretical work of Takagi and Nagase[7] that predicted a perpendicular orientation of the ligands, a long tin−tin distance of 2.900 Å, and a Sn−Sn−C bending angle of 111° (there is also a twist angle of 125.2°) for Ar*SnSnAr*. Note that this structure is only ca. 5 kcal·mol^{-1} higher in energy than a configuration in which the core is almost planar, and there is a very long 3.087 Å Sn−Sn bond with a 99° bending angle. Furthermore, recent calculations for the simple MeSnSnMe model system predicted a very similar planar CSnSnC framework with a longer 3.06 Å Sn−Sn bond and a 100° bending angle.[21] It seems probable that both Ar′SnSnAr′ and Ar*SnSnAr* have very similar structures in solution since the ultraviolet−visible spectra of the two compounds are almost identical. However, it is important to note that the degree of bending of Ar′SnSnAr′ or Ar*SnSnAr* in solution is not established experimentally. These findings for the various tin systems are also consistent with the computational work of Frenking and co-workers on Ar*PbPbAr* and related species which showed that the geometrical parameters at lead can be easily distorted.[22]

Conclusions

The ^{119}Sn solid-state NMR and Mössbauer data provide evidence that Ar′SnSnAr′ and Ar*SnSnAr* possess different solid-state structures although they appear to have similar structures in solution phase. Computational data have predicted that there is a very low energy penalty for large changes in the bending angle and Sn−Sn bond length in such compounds.[21] The low energy value suggests that geometries in such molecules can be affected by packing forces. Both the NMR and Mössbauer results suggest that in the crystalline phase the structure of Ar*SnSnAr* is more trans-bent and has a longer Sn−Sn bond than those measured for Ar′SnSnAr′ by X-ray diffraction. Suitable manipulation of the ligand substituents may allow a range of such structures to be crystallized and eventually characterized in detail by X-ray crystallographic methods.

Acknowledgment. The authors are indebted to the National Science Foundation for support, A. Aharoni for careful sample transfer using inert glovebox techniques, and to W. Glaberson and M. Brettschneider for the use of their DASWIN temperature monitoring program. We also thank Professors S. Nagase and A. Sekiguchi for useful discussions.

IC060983M

(21) Jung, Y.; Brynda, M.; Power, P. P.; Head-Gordon, M. *J. Am. Chem. Soc.* **2006**, *128*, 7185.
(22) Chen, Y.; Hartmann, M.; Diedenhofen, M.; Frenking, G. *Angew. Chem., Int. Ed.* **2001**, *40*, 2052.